Int. J. Heat Mass Transfer. Vol. 34, No. 4/5, pp. 1237–1248, 1991
Printed in Great Britain

0017–9310/91 $3.00+0.00

Natural convection and conduction in Trombe wall systems

R. BEN YEDDER and E. BILGEN†
Ecole Polytechnique, P.O. Box 6079, St. A Montreal, P.Q., Canada H3C 3A7

(*Received* 13 *March* 1990 *and in final form* 21 *June* 1990)

Abstract—The thermal performance of classical Trombe wall solar collector systems is studied numerically. It is assumed that the flow is laminar and two-dimensional, the glazing is isothermal and the solar heat absorbed by the wall is transferred to the air in the channel with a constant flux by natural convection and to the adjacent room by conduction and then by convection. The mass, momentum and energy conservation equations are discretized and solved using the finite difference–control volume method. Flow and temperature fields are produced and the results are presented in terms of temperature and velocity distributions in various parts of the system; the Nusselt number and the system thermal performance as a function of the Rayleigh number are also evaluated and presented.

1. INTRODUCTION

THE CLASSICAL Trombe wall solar collector system consists of a massive wall installed at a small distance from a glazing. The wall absorbs solar radiation and transmits part of it into the dwelling by natural convection through the solar chimney formed by the glazing on one side and the wall on the other. The air circulates through the vents at the bottom and top of the wall into the adjacent room. The natural convection is then controlled by these vents. The typical system dimensions are: 1.0–2.0 m high collector system, a distance of about 0.10 m between the glazing and the wall, 0.20–0.30 m thick wall, a vent size of about 70% of the chimney cross-section and about 3.0 m room width. The experimental studies indicate that the glazing temperature is quasi-isothermal and the wall releases heat to the air with a constant heat flux resulting in a surface temperature gradient along the solar chimney [1]. The advantages and the problems associated with this system are discussed elsewhere [2].

A review of the literature indicates that previous analyses are related to two major categories with various boundary conditions: (1) those that concern the natural convection between two parallel plates simulating the solar chimney; (2) those that concern the heat transfer in the entire system including the Trombe wall collector and the adjacent room.

In the first category, the case with symmetrically heated isothermal plates was studied by Bodoia and Osterle [3], the one with asymmetrically heated isothermal plates by Aung *et al.* [4], Aihara [5] and Akbari and Borgers [6], the problem with uniform wall heat fluxes by Aung *et al.* [4] and that with non-isothermal walls by Rheault and Bilgen [7]. In the second category, the case with both glazing and wall at isothermal conditions was studied by Ormiston *et al.* [8].

The review shows that the studies in the first category were only concerned with the convection in the chimney without considering the inlet and outlet conditions; in the study of the second category, the wall was assumed to be isothermal and also the effects of the conduction through the wall and of the vent positions and sizes were neglected. The present study models the natural convection in the entire system with more realistic boundary and operating conditions; it includes the vents as orifices with practical sizes, wall conduction and constant heat flux on the massive wall surface. It also examines the effect of geometrical parameters such as orifice size, its distance from the bounding horizontal surfaces, the distance between the massive wall and the wall opposite to it and the effect of the wall conductivity.

2. PROBLEM DESCRIPTION

The simplified Trombe wall system consisting of the collector, massive wall and the room is shown in Fig. 1. The solar radiation through the glazing strikes the massive wall surface and heats it up. The wall, cooled by natural convection of air in the channel, is usually at a higher temperature than the glazing. It releases part of the absorbed solar heat at constant flux to the air which circulates through the vents into the adjacent room. The other part is transmitted to the room by conduction. The glazing which is in contact with the outside air is at a constant temperature of T_1. The room is adjacent to the other parts of the dwelling at the same temperature; therefore it is assumed that the ceiling and the floor are adiabatic and that the heat gained by the room is dissipated through a fictive surface at a constant temperature of T_2 which is identical to the wall opposite to that of

† Author to whom all correspondence should be addressed.

NOMENCLATURE

A	aspect ratio, H/L
b	vent width [m]
B	vent size parameter, b/S
C	dimensionless lintel height, h/H
D	dimensionless chimney width, S/L
g	acceleration due to gravity [m s^{-2}]
H	cavity height [m]
h	lintel height [m]; convection coefficient [W m^{-2} K^{-1}]
k	thermal conductivity [W m^{-1} K^{-1}]
k_r	thermal conductivity ratio, k_{wall}/k_{fluid}
l	dimensionless vent size, $(y-H+b+h)/b$
L	cavity width [m]
Nu	Nusselt number, hL/k
P	dimensionless pressure
p	pressure [Pa]
Pr	Prandtl number, ν/α
Q	flow rate through the vents, $\int_0^1 U\,\mathrm{d}b$
q	heat flux [W m^{-2}]
Ra	Rayleigh number, $g\beta L^4 q/\nu\alpha k$
S	width of the chimney [m]
T	temperature [K]
ΔT	temperature difference between the outer walls, T_1-T_2 [K]
u, v	fluid velocity in the x- and y-direction [m s^{-1}]
U, V	dimensionless fluid velocities
x, y	Cartesian coordinates
X, Y	dimensionless distance on x- and y-axis.

Greek symbols

α	thermal diffusivity [m^2 s^{-1}]
β	thermal expansion of fluid [K^{-1}]
η	efficiency
θ	dimensionless temperature
μ	dynamic viscosity [kg m^{-1} s^{-1}]
ν	kinematic viscosity [m^2 s^{-1}]
ρ	fluid density [kg m^3].

Subscripts

1	left wall or glazing; left channel
2	right wall or fictive wall; right channel.

the massive wall. By considering the heat transfer by natural convection of air and conduction through the massive wall, the problem can be reduced to the one shown in Fig. 1: two horizontal boundaries are adiabatic. Two vertical bounding surfaces are isothermal at different temperatures of T_1 and T_2. The massive wall surface in the chimney releases heat with a constant flux. Depending on the density of heat flux from the massive wall and the boundary conditions on the two vertical surfaces, various convection modes and hence heat transfer result.

The geometrical parameters are chosen based on the Trombe wall system applications: $A = H/L$ from 0.7 to 1.0, $D = S/L = 1/33$, $d/L = 2/33$, $B = b/S$ from 0.0 (corresponding to the Trombe wall without vents) to 2.25 and $C = h/H$ from 0.0 to 1/23. The thermophysical parameters are Ra from 10^7 to 2×10^8, $\Delta T = T_1 - T_2$ from -10 to 10°C and $k_r = k_{wall}/k_{air} = 20$ (corresponding to concrete wall) and 100 (corresponding to stone wall).

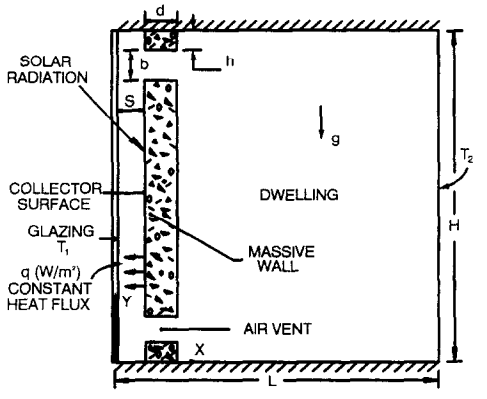

FIG. 1. Problem description, geometrical parameters and coordinate system.

3. MATHEMATICAL MODEL AND NUMERICAL METHOD

The mathematical model and the computer code are developed for a general case to study natural convection in cavities which may be partially divided and may contain several walls with different conductivity. The flow is assumed to be steady, laminar and two-dimensional. The Boussinesq approximation is used to account for the density variation. The mathematical model is briefly described below.

Governing equations are

$$\frac{\partial u}{\partial x}+\frac{\partial v}{\partial y}=0 \tag{1}$$

$$u\frac{\partial u}{\partial x}+v\frac{\partial u}{\partial y}=-\frac{1}{\rho}\frac{\partial p}{\partial x}+\nu\nabla^2 u \tag{2}$$

$$u\frac{\partial v}{\partial x}+v\frac{\partial v}{\partial y}=-\frac{1}{\rho}\frac{\partial p}{\partial y}+\nu\nabla^2 v-g[1-\beta(T-T_1)] \tag{3}$$

$$u\frac{\partial T}{\partial x}+v\frac{\partial T}{\partial y}=\alpha\nabla^2 T \tag{4}$$

by introducing the following non-dimensional variables:

$$X=\frac{x}{L},\quad Y=\frac{y}{L} \tag{5}$$

$$U=\frac{uL}{\nu},\quad V=\frac{vL}{\nu} \tag{6}$$

$$P=\frac{p+\rho gy}{\rho(\nu/L)^2},\quad \theta=\frac{T-T_1}{\frac{Lq}{k}}. \tag{7}$$

Following Patankar [9], two coefficients are introduced and the resulting non-dimensional continuity, momentum and energy equations are obtained as follows:

$$\frac{\partial U}{\partial X}+\frac{\partial V}{\partial Y}=0 \tag{8}$$

$$U\frac{\partial U}{\partial X}+V\frac{\partial U}{\partial Y}=-\frac{\partial P}{\partial X}+\Gamma\nabla^2U \tag{9}$$

$$U\frac{\partial V}{\partial X}+V\frac{\partial V}{\partial Y}=-\frac{\partial P}{\partial Y}+\Gamma\nabla^2V+\frac{Ra}{Pr}\theta \tag{10}$$

$$U\frac{\partial \theta}{\partial X}+V\frac{\partial \theta}{\partial Y}=\frac{K}{Pr}\nabla^2\theta \tag{11}$$

where Γ is a general diffusion coefficient which is equal to 1 in the fluid region and 10^{15} in the solid region, and K a thermal conductivity ratio which is equal to 1 in the fluid region and k_r in the solid region.

The energy balance at the wall–fluid interface at $x = S$ requires

$$\frac{\partial \theta}{\partial X}=1. \tag{12}$$

The boundary conditions are the no-slip conditions on all the rigid wall surfaces, isothermal temperature on the vertical end walls and adiabatic on the horizontal walls. Hence, the boundary conditions for this problem are (see Fig. 1)

$$\left.\begin{array}{ll} X=0,\ 0\leqslant Y\leqslant A & U=V=0;\ \theta=\theta_1 \\ X=1,\ 0\leqslant Y\leqslant A & U=V=0;\ \theta=\theta_2 \\ 0\leqslant X\leqslant 1,\ Y=0, A & U=V=0;\ \dfrac{\partial\theta}{\partial Y}=0 \\ X=D,\quad \begin{array}{l} 0\leqslant Y\leqslant C \\ C+B\cdot D\leqslant Y\leqslant A-(C+B\cdot D) \\ A-C\leqslant Y\leqslant A \end{array} & \dfrac{\partial\theta}{\partial X}=1. \end{array}\right\} \tag{13}$$

The numerical method used to solve the system of equations (8)–(11) is the SIMPLER method [9]. This algorithm is based on a control volume approach, and the equations are discretized by ensuring that conservation of mass, momentum and energy are satisfied over each control volume. A staggered grid for velocity is used, as suggested by Patankar, to avoid wavy pressure and velocity fields.

It should be noted that the conduction in the massive wall is accounted for by introducing the dimensionless parameter K in the discretized non-dimensional energy equation (11). By definition, it is equal to 1 in the fluid region and to $k_r = k_{wall}/k_{air}$ in the solid region. In addition, Γ is specified as 1 in the fluid region and 10^{15} in the solid region. The latter ensures that $U = V = 0$ everywhere in the solid region including the solid–fluid interface. The heat flux from other surfaces of the wall is deduced from the results of the computation.

4. VALIDATION OF THE CODE AND COMPUTATION

The computer code based on the mathematical model above and the SIMPLER method is validated for various cases: square cavity, rectangular cavity with aspect ratio of 5 and rectangular cavity with aspect ratio of 10. The comparison of various parameters for a square cavity and the average Nusselt number as a function of the Rayleigh number for rectangular cavities are presented in ref. [10]. It was seen that for all the cases tested the present code produced results in agreement with those published in the literature.

A non-uniform grid size was used to solve the present problem. The relative number of grids in the solar chimney, air vents and the massive wall was about 20% of the total. This ensured enough details on the flow and temperature fields in these regions. After several tries and comparisons with the test cases discussed above, it was found that a 25×25 grid size ensured independence of solution on the grid with reasonable computation time. For small Rayleigh numbers, the number of iterations was about 35. For larger Ra, the solution for smaller Ra was used to initialize the computation so the number of iterations was reduced considerably. The relaxation parameter, as defined in ref. [9], was varied from 0.50 for small Ra to about 0.40 for large Ra. The execution time for a typical case with $Ra = 5\times10^6$ and 20 iterations was 12 CPU seconds on an IBM 3090 with 17 mips.

The convergence criterion was based on the corrected pressure field. When the corrected terms were small enough so that no difference existed between the pressure fields before and after correction, the computation was stopped. Hence

$$\sum_{i=1}^{i_{max}}\sum_{j=1}^{j_{max}} b_{ij}\leqslant\varepsilon \tag{14}$$

where b_{ij} is the source term in the pressure correction equation [9] and $\varepsilon\leqslant0.001$.

In addition to the usual accuracy control, the accuracy of computations was controlled using the energy conservation within the system. It was found that it was accurate within 0.1% in the worst case.

5. RESULTS AND DISCUSSION

Various computations were carried out using the range of geometrical parameters discussed earlier for Ra from 10^7 to 2.0×10^8 and ΔT from -10 to 10°C. The reason for using ΔT in its dimensional form is to

have a better insight in Trombe wall applications. A positive ΔT corresponds to a warm glazing which happens usually when the solar radiation strikes the collector surface. This is the favorable condition for a positive (or useful) convection in the solar chimney. A negative ΔT corresponds, on the other hand, to a cooler glazing temperature, possibly with an inverse circulation in the chimney. The results were reduced to carry out parametric studies on the influence of various dimensionless parameters: temperature distribution θ in the x- and y-directions of the solar chimney, the Nusselt and Rayleigh numbers. First, the case with $A = 1.0$, $B = 2.25$, $C = 1/23$ and $k_r = 20$ will be presented in detail; then, the effects of A, B, C and k_r will be discussed.

5.1. *Case with* $A = 1$, $B = 2.25$, $C = 1/23$ *and* $k_r = 20$

The massive wall surface temperature along the chimney as a function of Y is shown in Fig. 2 for $\Delta T = -10$ and 10°C and for various Ra. The non-dimensional surface temperature is nonlinear. Because of the definition of the non-dimensional temperature, higher values of θ do not necessarily indicate higher surface temperatures. In fact, as it will be discussed later, the clockwise air circulation is achieved for lower values of mean θ. This is due to the definition of θ in equation (7) which states that θ is inversely proportional to q.

The temperature and velocity distributions at solar chimney mid-height and along x, with x/S from 0 to 1 are presented in Fig. 3 for $\Delta T = -10$°C and in Fig. 4 for $\Delta T = 10$°C and for various Rayleigh numbers. Following the definition of ΔT, the negative value indicates a lower glazing temperature and a positive value at higher temperature with respect to the room fictive wall temperature. Figure 3 indicates for $\Delta T = -10$°C the temperature profile in the chimney mid-height is an increasing function of the chimney width and Ra. For low Ra, the flow is from top to bottom and with the vents open, the system loses energy from the room. As Ra increases, the flow becomes reversed near the wall. For the highest Ra computed, the net flow is from the chimney to the room indicating that the heat flux from the massive wall must exceed a threshold value in order to have a positive (or useful) circulation in the solar chimney. Figure 4 shows the same parameters for $\Delta T = 10$°C. In this case as the glazing temperature is higher than the room fictive wall temperature, the air temperature decreases along the chimney for low Ra; it becomes an increasing function with x/S at higher Ra. The velocity profile indicates velocities in the positive y-direction without a back flow. This is the typical case of the Trombe wall operation during the sunshine hours: due to radiation heat exchange with the massive wall, the glazing temperature is higher than those of the room wall surfaces. The velocity profiles at the top vent for $\Delta T = -10$ and 10°C and various Ra are presented in Fig. 5. The results on the right for $\Delta T = -10$°C correspond to Fig. 3 and those on the left for $\Delta T = 10$°C to Fig. 4. The flow rates are negative for the first case at $Ra = 10^7$ and 10^8 then positive at $Ra = 2 \times 10^8$ confirming the results of Fig. 3. They are all positive in the second case although there is a small back flow on the upper part of the vent at high Ra. These results are also in agreement with those in Fig. 4.

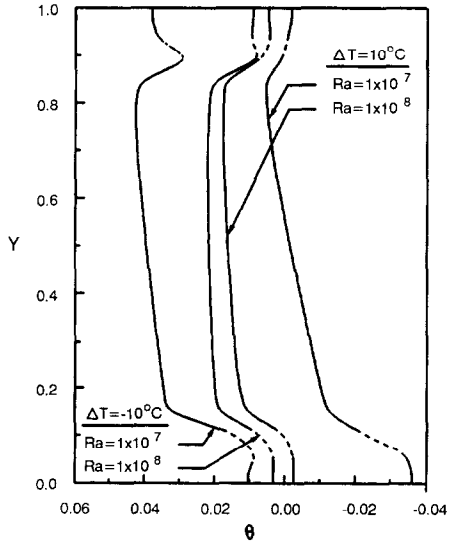

FIG. 2. Temperature variation along the height at the massive wall as a function of the Rayleigh number and for $\Delta T = -10$ and 10°C. Dashed curves correspond to the vent locations and indicate the air temperature. Other parameters are $A = 1$, $B = 2.25$, $C = 1/23$ and $k_r = 20$.

The heat transfer from the left (i.e. glazing) and right (i.e. fictive wall) bounding sides is calculated as

$$Nu = \frac{1}{\theta_2}\int_0^1 \frac{\partial \theta}{\partial X}\,\mathrm{d}Y. \tag{15}$$

The results are reduced as Nusselt numbers Nu_1 and Nu_2 are presented as a function of Ra for two ΔT values in Fig. 6. The positive Nu indicates a heat flow in the positive X-direction. The negative values of Nu_1 and positive values of Nu_2 indicate a loss from the system. The sum of the heat fluxes from the two bounding surfaces, the glazing on the left and the room fictive wall on the right, should be equal to the heat flux from the surfaces of the massive wall. Since the definition of the Rayleigh number contains the heat flux from the massive wall, the absolute values of Nu_1 and Nu_2 are an increasing function of Ra. Figure 6 shows that at low Ra the heat may be gained through the glazing when $\Delta T = 10$°C and through the room fictive wall when $\Delta T = -10$°C. Generally, however, the heat is lost through both surfaces at high Ra. The heat loss is higher through the glazing than the room fictive wall.

Thermal performance of the system defined as the ratio of the useful to total energy is

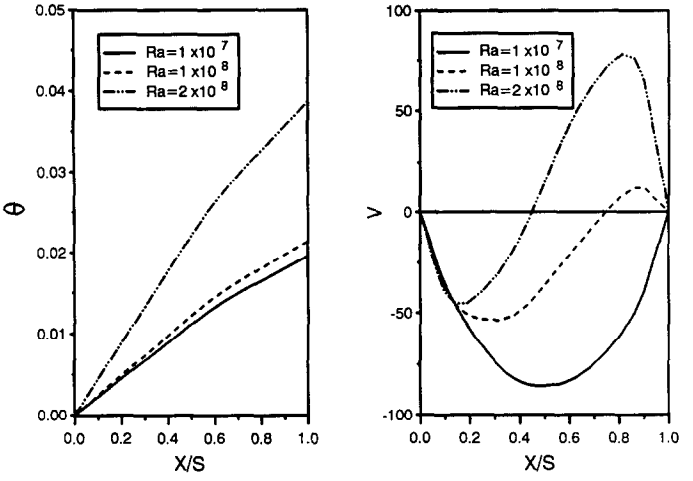

FIG. 3. Temperature (on the left) and velocity (on the right) at the chimney mid-height ($Y = 0.5$) for various Rayleigh numbers and $\Delta T = -10°C$. Other parameters are $A = 1$, $B = 2.25$, $C = 1/23$ and $k_r = 20$.

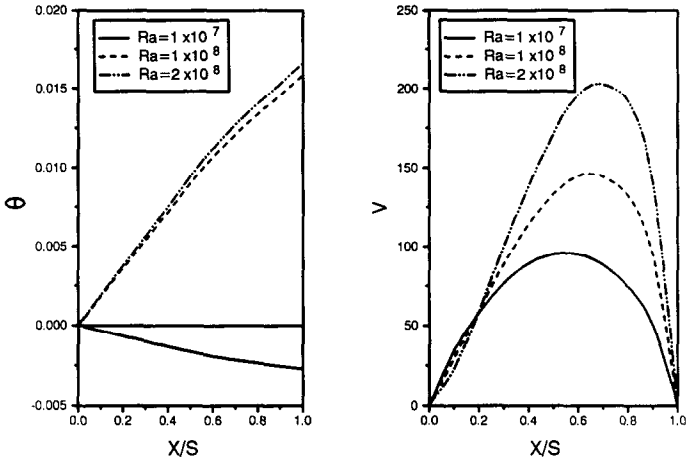

FIG. 4. Temperature (on the left) and velocity (on the right) at the chimney mid-height ($Y = 0.5$) for various Rayleigh numbers and $\Delta T = 10°C$. Other parameters are $A = 1$, $B = 2.25$, $C = 1/23$ and $k_r = 20$.

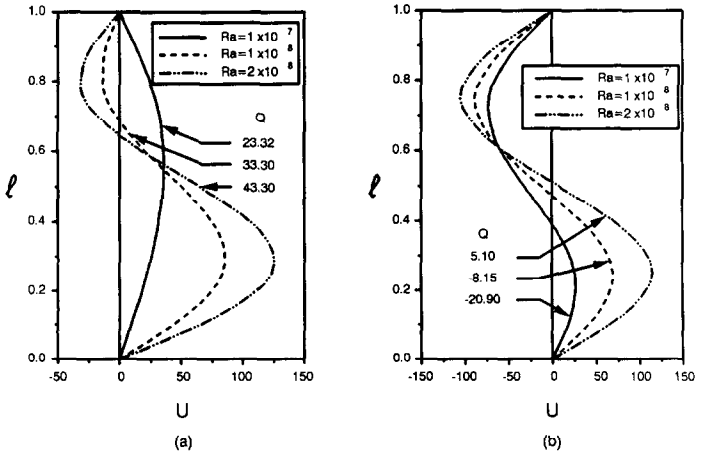

FIG. 5. Velocity profile at the top vent for various Rayleigh numbers: (a) $\Delta T = 10°C$; (b) $\Delta T = -10°C$. Other parameters are $A = 1$, $B = 2.25$, $C = 1/23$ and $k_r = 20$.

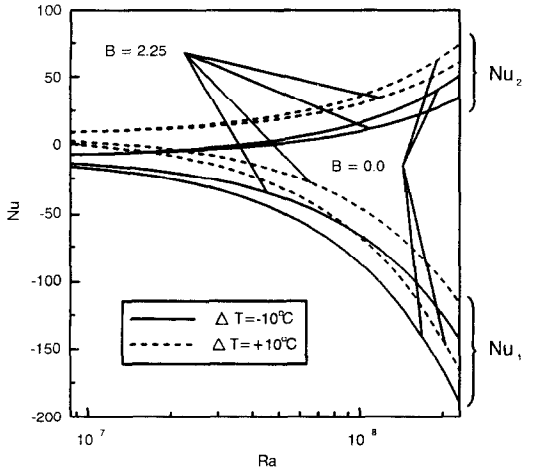

FIG. 6. Heat transfer through the bounding surfaces as a function of Rayleigh number for $\Delta T = -10$ and 10°C. Nu_1 is the heat transfer through the glazing and Nu_2 through the room fictive wall. Other parameters are $A = 1$, $B = 2.25$ with $C = 1/23$, $B = 0.0$ with C not defined and $k_r = 20$.

$$\eta = \frac{\int_0^A \left.\frac{\partial\theta}{\partial X}\right|_{X=1} \mathrm{d}Y}{\int_0^A \left.\frac{\partial\theta}{\partial X}\right|_{X=D} \mathrm{d}Y}. \qquad (16)$$

This is calculated for various Ra and two ΔT values and the results are presented in Fig. 7. It can be seen that the thermal efficiency of the system is an increasing function of Ra. The case with $\Delta T = 10$°C corresponding to a higher chimney temperature is more favorable for better performance of the system than with $\Delta T = -10$°C: the thermal efficiency is higher by about 45% at high Ra and about 100% at low Ra.

The ratio of energy transmitted to the dwelling by conduction through the massive wall to that by convection through the vents is also calculated for various Ra and for two ΔT values and the results are presented

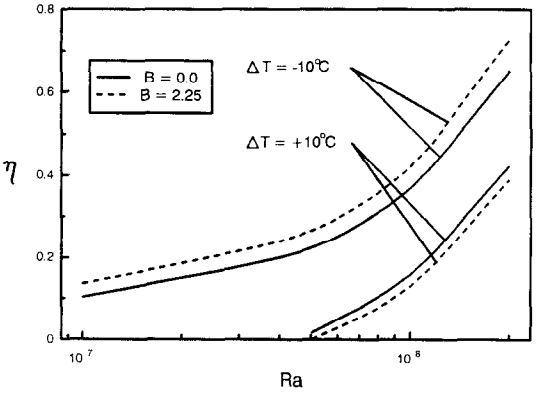

FIG. 7. Thermal performance of the system for $B = 2.25$ and 0.0. Other parameters are $A = 1$, $B = 2.25$ with $C = 1/23$, $B = 0.0$ with C not defined and $k_r = 20$.

Table 1. Ratio of energy transfer by conduction to convection for $B = 2.25$

	Ra		
	1×10^7	5×10^7	1×10^8
$\Delta T = 10$°C	2.33	3.06	18.11
$\Delta T = -10$°C	1.61	3.40	13.95

in Table 1. It can be seen that for low Ra this ratio has similar magnitudes and that it increases with increasing Ra. It is generally higher for high Ra and $\Delta T = 10$°C since the energy transfer by convection through the glazing (i.e. losses) is higher in this case and heat transfer by conduction is dominant.

The streamlines and isotherms in the system for $\Delta T = -10$ and 10°C and for two values of Ra are presented in Fig. 8 where the various conditions discussed earlier can also be observed. For $\Delta T = 10$°C the streamlines indicate a clockwise circulation, i.e. the heat is gained from the Trombe wall either by circulation through the chimney or from the inside surface of the massive wall by convection. As expected, the air circulation increases with increasing Ra. The isotherms on the right show the variation of $\Delta\theta$ in the system: for $Ra = 10^7$, $\Delta\theta$ varies from -0.0096 on the right wall surface to 0.0 on the glazing and similarly for $Ra = 10^8$ from -0.096 to 0.0. The isotherms in Fig. 8(a) are all negative indicating that the air temperature is inferior to the glazing temperature but higher than that of the fictive wall temperature. For $Ra = 10^8$ in Fig. 8(b) the lower part of the room is at temperatures lower than that of the glazing but the upper part is at higher temperatures. In both cases, the stratification of the room air is evident. For $\Delta T = -10$°C in Fig. 8(c) the streamlines at low Ra indicate a counter-clockwise circulation, i.e. a heat loss through the Trombe wall system. For higher Ra in Fig. 8(d) the air circulation becomes clockwise with most of the heat gains from the inside surface of the massive wall by convection. In this case, the formation of secondary cells on the lower and upper part of the room can also be noticed indicating a back flow through the vents. The isotherms for this case vary from 0.0 on the glazing to 0.096 on the room wall for $Ra = 10^7$ shown in Fig. 8(c) and from 0.0 to 0.0096 for $Ra = 10^8$ shown in Fig. 8(d). Again $\Delta\theta$ in both cases indicates a stratified room air and the temperatures are lower than those at the bounding surfaces. It is clear from these figures that in order to have an air circulation in the positive Y-direction (heat gain from the chimney) ΔT should be positive or if it is negative, Ra must be high enough to have clockwise circulation in the system. The threshold value can be inferred from Fig. 6 as about 3.6×10^7.

5.2. *Effect of A*

Computations were carried out with $A = 0.7$ and other parameters as in the previous case. $A = 0.7$ cor-

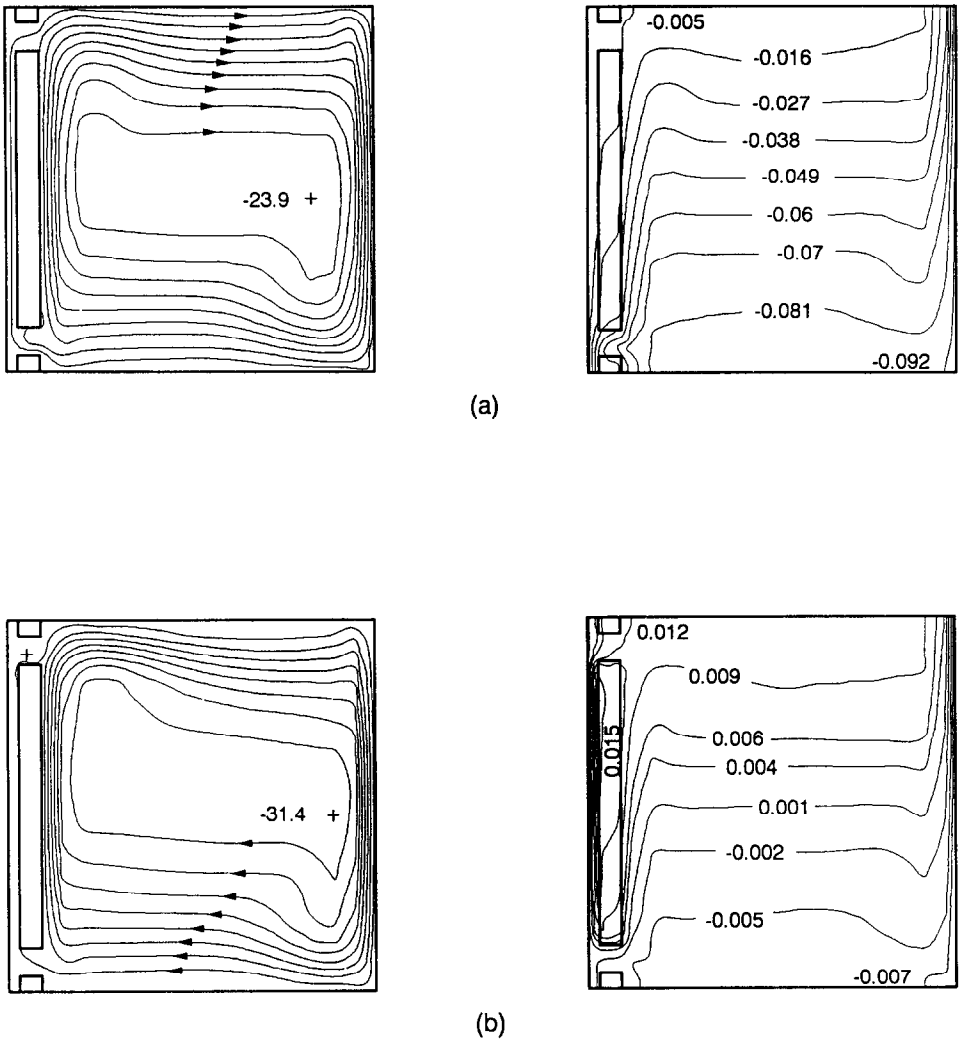

FIG. 8. Typical streamlines (on the left) and isotherms (on the right) for the case of: (a) $Ra = 10^7$, $\Delta T = 10$°C; (b) $Ra = 10^8$, $\Delta T = 10$°C; (c) $Ra = 10^7$, $\Delta T = -10$°C; (d) $Ra = 10^8$, $\Delta T = -10$°C. Other parameters are $A = 1$, $B = 2.25$, $C = 1/23$ and $k_r = 20$.

responds to a wider dwelling: with a typical $H = 2.80$ m, $A = 0.7$ corresponds to $L = 4.0$ m which may be an upper limit for Trombe wall applications. The results showed a negligible effect of A on various parameters. The heat transfer from the glazing, Nu_1, for $A = 0.7$ and 1.0 is presented in Table 2 for various Ra and ΔT.

Table 2. Heat transfer through the glazing for $A = 0.7$ and 1.0

	Nu_1			
	$\Delta T = -10$°C		$\Delta T = 10$°C	
Ra	$A = 0.7$	$A = 1.0$	$A = 0.7$	$A = 1.0$
1×10^7	−13.62	−13.57	2.39	2.30
5×10^7	−37.91	−37.96	−19.52	−19.63
1×10^8	−67.63	−67.84	−46.40	−46.50

It can be seen that the absolute value of Nu_1 increased for low Ra and decreased for high Ra. Since a negative Nu_1 indicates a loss through the glazing, it is seen that a Trombe system in a wider dwelling will perform slightly better at high Ra. Its performance will be slightly lower at low Ra.

5.3. *Effect of B*

Computations were carried out with $B = 0.0$ with other parameters as in the first case. A value of $B = 0.0$ corresponds to Trombe wall systems without vents. These are the most simple Trombe wall systems which do not require a control strategy or maintenance [11]. It should also be noted that in this case, the energy transfer from the system to the dwelling is by conduction only.

The temperature and velocity distributions at solar

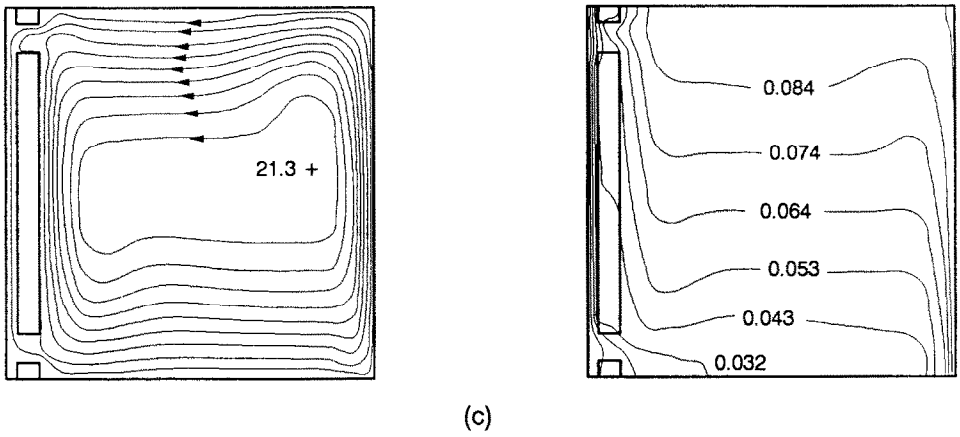

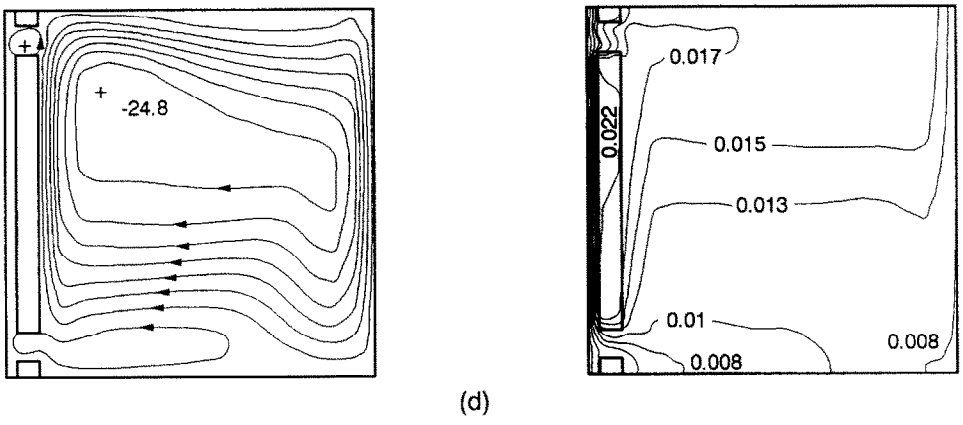

FIG. 8.—*Continued.*

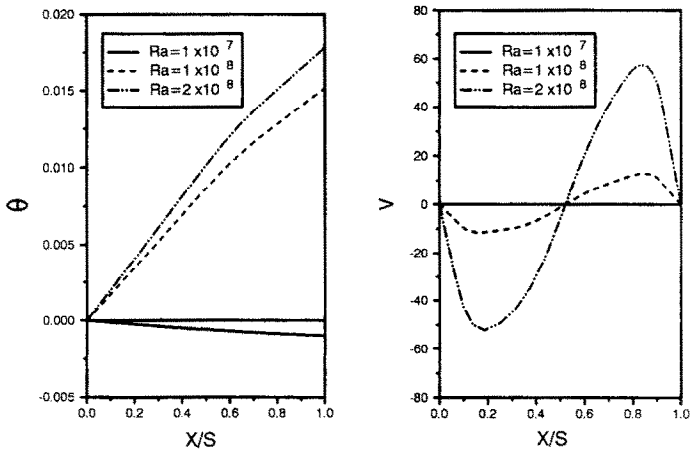

FIG. 9. Temperature (on the left) and velocity (on the right) at the chimney mid-height ($Y = 0.5$) for various Rayleigh numbers and $\Delta T = 10°C$. Other parameters are $A = 1$, $B = 0.0$ and $k_r = 20$.

chimney mid-height and along x, with x/S from 0 to 1 are presented in Fig. 9 for $\Delta T = 10°C$ and various Ra. As discussed earlier, $\Delta T = 10°C$ represents the favorable case for useful energy gain from the system. It can be seen that the temperature distribution is similar to that of the case with $B = 2.25$ in Fig. 4 and the same discussion and comments apply. The velocity distribution is, however, one in a long rectangular cavity: the air is heated at the massive wall, it circulates at the top and cooled down at the glazing; it circulates again from the bottom of the cavity. As expected, the circulation is stronger as Ra increases.

The overall situation can be seen in Fig. 10 where the streamlines and isotherms in the system are plotted for $Ra = 10^7$ and 10^8 and $\Delta T = 10$ and $-10°C$. For $\Delta T = 10°C$ in Figs. 10(a) and (b), the circulation in the dwelling is clockwise, i.e. heat is gained from the massive wall; there is a stratification of air in the dwelling. The air circulation is increased with increasing Ra. The negative values on isotherms indicate an air temperature lower than that of glazing; it is seen in Fig. 10(b) that the air temperature in the dwelling becomes higher than that of glazing at higher elevation and high Ra. In Figs. 10(c) and (d), the isotherms on the right show that the fictive wall temperature is higher than that of the glazing as ΔT is negative in this case. In Fig. 10(c) at low Ra, the air circulation is anti-clockwise indicating a heat transfer from the fictive wall through the massive wall to the glazing. In Fig. 10(d) at higher Ra, the air circulation is again clockwise with a heat gain from the massive wall to the dwelling.

The heat transfer through the glazing and the fictive wall as a function of Ra and for various ΔT values is

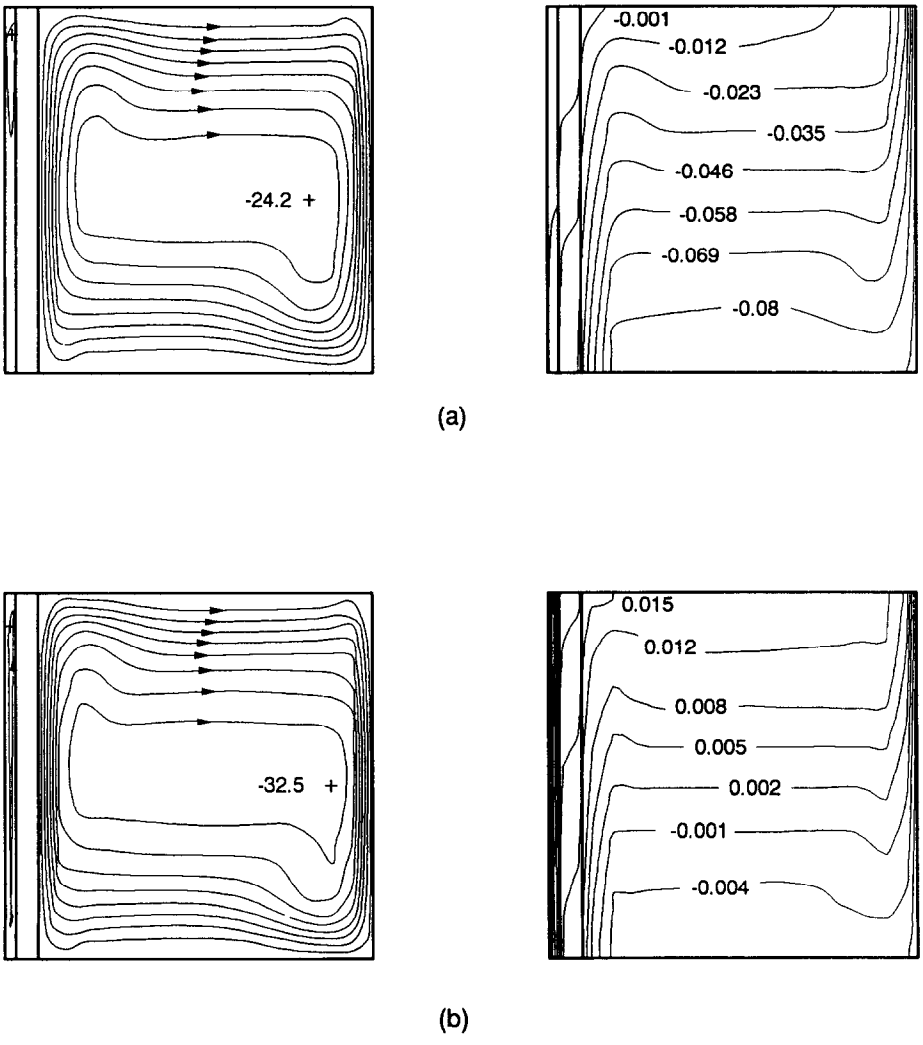

FIG. 10. Typical streamlines (on the left) and isotherms (on the right) for the case of: (a) $Ra = 10^7$, $\Delta T = 10°C$; (b) $Ra = 10^8$, $\Delta T = 10°C$; (c) $Ra = 10^7$, $\Delta T = -10°C$; (d) $Ra = 10^8$, $\Delta T = -10°C$. Other parameters are $A = 1$, $B = 0.0$ and $k_r = 20$.

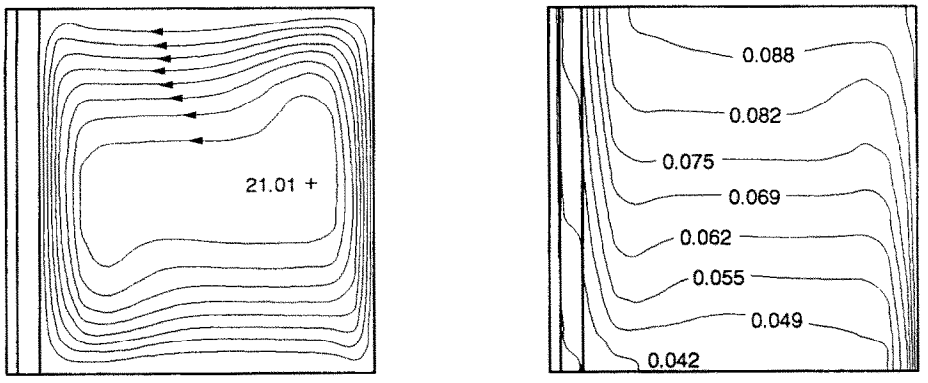

(c)

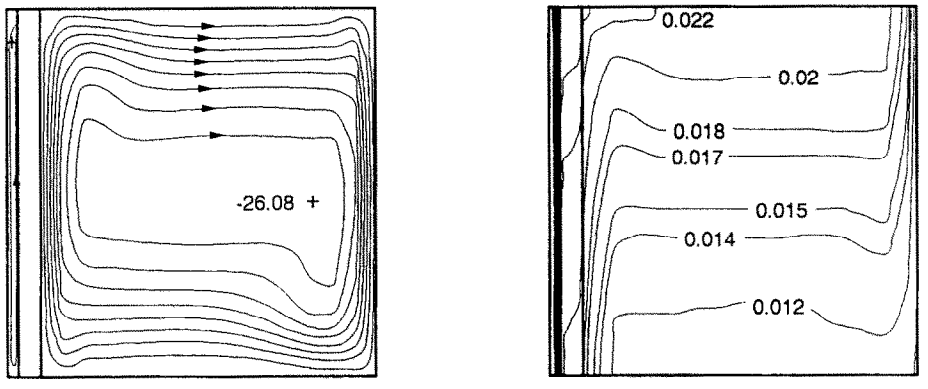

(d)

FIG. 10.—*Continued.*

also shown in Fig. 6 for this case. The increased negative Nu_1 (i.e. the losses through the glazing) and Nu_2 (i.e. the losses through the fictive wall) for both ΔT, in comparison with the first case indicates that the massive wall without vents is a better insulating barrier for heat losses from the dwelling through the massive wall system. The losses from the glazing are by convection and the gain from the system is only by conduction through the wall which is lost through the fictive wall.

The thermal performance of this system is calculated in a similar manner as for the first case and the results are also shown in Fig. 7. It is seen that for $\Delta T = 10°C$, the system with vents performs better than that without vents by about 25% at low Ra and 10% at high Ra; the reason is that the thermal losses from the glazing are higher for the system without vents as can also be seen in Fig. 6. For $\Delta T = -10°C$, the system without vents performs much better than that with vents since the massive wall prevents losses by convection from the dwelling through the system.

5.4. *Effect of C*

Computations were carried out with $C = 0.0$ and other parameters as in the first case. $C = 0.0$ corresponds to vents with their upper and lower edges flush with the ceiling and floor, respectively. The heat transfer through the glazing, Nu_1, for $C = 0.0$ and 1/23 is presented in Table 3 for various Ra and ΔT. It is seen that the performance of the system is decreased by a maximum of 1% for $\Delta T = -10°C$ and that the system performs better in the more favorable case of $\Delta T = 10°C$; the improvement is about 10% at low Ra indicating that the air circulation by natural convection through the vents is increased due to better geometrical conditions.

Table 3. Heat transfer through the glazing for $C = 0.0$ and 1/23

	Nu_1			
	$\Delta T = -10°C$		$\Delta T = 10°C$	
Ra	$C = 0$	$C = 1/23$	$C = 0$	$C = 1/23$
1×10^7	−13.70	−13.57	2.53	2.30
5×10^7	−38.22	−37.96	−19.37	−19.63
1×10^8	−68.15	−67.84	−46.40	−46.50

5.5. *Effect of* k_r

Computations were carried out with $k_r = 100$ with other parameters as in the first case, except that $B = 0.0$. $k_r = 100$ corresponds to stone and similar materials used in Trombe walls. The results indicated a non-negligible effect of wall conductivity on various parameters discussed earlier: for $\Delta T = -10°C$, the temperature in the system (chimney, wall and dwelling) is increased by about 1.96% at low and 19.37% at high Ra. The heat transfer, Nu_2, representing the useful energy gain through the glazing, is increased, for $\Delta T = -10°C$, by about 1% at low Ra and 1.9% at high Ra; for $\Delta T = 10°C$, it increased by 1.4 and 2.2%, respectively.

6. CONCLUSIONS

The thermal performance of the classical Trombe wall collector system including solar collector and the adjacent room has been studied numerically. Following experimental studies and practical applications of the system, the geometrical parameters and boundary conditions are chosen and parametric studies are presented. The results indicate that the temperature difference ΔT and the Rayleigh number are two important parameters affecting the heat transfer: in order to have a useful energy from the solar collector system either ΔT must be positive or if it is negative, the Rayleigh number, hence the heat flux from the massive wall, must be higher than a threshold value. The systems without vents perform better than those with vents during sunshine hours, both better still when the wall conductivity is high.

Acknowledgement—Financial support from the Natural Sciences and Engineering Council Canada is acknowledged.

REFERENCES

1. S. A. Betrouni, Z. Zrikem and E. Bilgen, On the free convection heat transfer within the Trombe–Michel wall collector system, *2nd ASME/JSME Thermal Engng Conf., Proc. Solar Engng 1987*, Vol. 2, pp. 970–975 (1987).
2. E. Bilgen and J. Michel, Integration of solar systems in architectural and urban design. In *Solar Energy Application in Buildings* (Edited by A. A. M. Sayigh), Chap. 19, pp. 389-422. Academic Press, New York (1979).
3. J. R. Bodoia and J. F. Osterle, The development of free convection between heated vertical plates, *J. Heat Transfer*, **C84,** 40–44 (1962).
4. W. Aung, L. S. Fletcher and V. Sernas, Developing laminar free convection between vertical flat plates with asymmetric heating, *Int. J. Heat Mass Transfer* **15,** 2293–2308 (1972).
5. T. Aihara, Effects of inlet boundary-conditions on numerical solutions of free convection between vertical parallel plates, *Rep. Inst. High Speed Mech., Tohoku Univ.* **28,** 1–27 (1973).
6. H. Akbari and T. R. Borgers, Free convective laminar flow within the Trombe wall channel, *Solar Energy* **22,** 165–174 (1979).
7. S. Rheault and E. Bilgen, Developing laminar convection between non-isothermal vertical parallel plates, *Proc. ASME Heat Transfer 1988* (Edited by K. T. Yang), 3, HTD-Vol. 104, pp. 103–108 (1988).
8. S. J. Ormiston, G. D. Raithby and K. G. T. Hollands, Numerical predictions of natural convection in a Trombe wall system, *Int. J. Heat Mass Transfer* **29,** 869–877 (1986).
9. S. V. Patankar, *Numerical Heat Transfer and Fluid Flow*. Hemisphere, New York (1980).
10. R. Ben Yedder, Z.-G. Du and E. Bilgen, Heat transfer by natural convection in composite Trombe wall solar collector, *Proc. ASME WA, Solar Energy Technology—1989*, San Francisco, 10–15 December (Edited by J. T. Beard and H. C. Hewitt, Jr.), SED-Vol. 8, pp. 7–13 (1989).
11. Z. Zrikem and E. Bilgen, Theoretical study of a composite Trombe–Michel wall solar collector system, *Solar Energy* **39**(5), 409–419 (1987).

CONVECTION NATURELLE ET CONDUCTION DANS LES SYSTEMES A MUR TROMBE

Résumé—On étudie numériquement les performances thermiques des systèmes collecteurs classiques à un mur Trombe. On suppose que l'écoulement est laminaire et bidimensionnel, le vitrage est isotherme et la chaleur solaire absorbée par la paroi est transférée à l'air dans le canal avec un flux constant, par convection naturelle et à la pièce adjacente par conduction puis par convection. Les équations de masse, quantité de mouvement et énergie sont discrétisées et résolues en utilisant la méthode des différences finies et des volumes de contrôle. Les champs de vitesse et de température sont obtenus et les résultats sont présentés pour les différentes parties du système; le nombre de Nusselt et les performances thermiques du système sont évalués et présentés en fonction du nombre de Rayleigh.

NATÜRLICHE KONVEKTION UND WÄRMELEITUNG IN EINEM TROMBEWANDSYSTEM

Zusammenfassung—Das thermische Verhalten des klassichen Sonnenkollektorsystems einer Trombewand wird numerisch untersucht. Dabei werden folgende Annahmen getroffen: Die Strömung ist laminar und zweidimensional, die Verglasung ist isotherm, die von der Wand absorbierte Sonnenstrahlung wird an die Luft im Kanal durch natürliche Konvektion (konstante Wärmestromdichte) und an den benachbarten Raum durch Wärmeleitung und dann durch Konvektion übertragen. Die Erhaltungsgleichungen für Masse, Impuls und Energie werden diskretisiert und mit einem Finite-Differenzen-Verfahren für die Kontrollvolumina gelöst. Dabei werden Strömungs- und Temperaturfelder berechnet und für die verschiedenen Teile des Systems dargestellt. Die Nusselt-Zahl und das thermische Verhalten des Systems werden ebenfalls berechnet und als Funktion der Rayleigh-Zahl dargestellt.

ЕСТЕСТВЕННАЯ КОНВЕКЦИЯ И ТЕПЛОПРОВОДНОСТЬ В СИСТЕМАХ СТЕНОК ТРОМБА

Аннотация—Численно исследуются тепловые характеристики классических систем стенок Тромба в коллекторах солнечной энергии. Предполагается, что течение является ламинарным и двумерным, остекление—изотермическим и поглощаемая стенкой солнечная энергия по каналу с постоянным тепловым потоком передается в воздух естественной конвекцией, а в окружающее помещение—теплопроводностью и конвекцией. Уравнения сохранения массы, количества движения и энергии решаются конечно-разностным методом. Определяются поля скоростей и температур, полученные результаты приводятся в виде распределений температур и скоростей в различных частях системы. Оцениваются и приводятся также число Нуссельта и тепловые характеристики системы в зависимости от числа Рэлея.